

Evolution of separate screening soliton pairs in a biased series photorefractive crystal circuit

Jinsong Liu* and Zhonghua Hao†

State Key Laboratory of Laser Technology, Huazhong University of Science and Technology, Wuhan, Hubei 430074, People's Republic of China

(Received 21 November 2001; published 7 June 2002)

This paper presents calculations for an idea in photorefractive spatial soliton, namely, screening solitons form in a biased series photorefractive crystal circuit consisting of two photorefractive crystals connected electronically by electrode leads in a chain with a voltage source. A system of two coupled equations is derived under appropriate conditions for two-beam propagation in the crystal circuit. The possibility of obtaining steady-state bright and dark screening soliton solutions is investigated in one dimension and, the existence of dark-dark, bright-dark, and bright-bright separate screening soliton pairs in such a circuit is proved. The numerical results show that the two solitons in a soliton pair can affect each other by the light-induced current and their coupling can affect their spatial profiles, dynamical evolutions, stabilities, and self-deflection. Under the limit in which the optical wave has a spatial extent much less than the width of the crystal, only the dark soliton can affect the other soliton by the light-induced current, but the bright soliton cannot. For a bright-dark or dark-dark soliton pair, the dark soliton in a weak input intensity can be obtained for a larger nonlinearity than for a stronger input intensity. For a bright-dark soliton pair, increasing the input intensity of the dark soliton can increase the bending angle of the bright soliton. Some potential applications are discussed.

DOI: 10.1103/PhysRevE.65.066601

PACS number(s): 42.65.Tg, 42.65.Hw

I. INTRODUCTION

Investigation of spatial solitons is considered to be important because of their possible applications for optical switching and routing, in which photorefractive (PR) solitons have been a topic of considerable interest in the last decade [1–17]. To date, a quasi-steady-state soliton has been predicted [1] and found experimentally [2] and three different kinds of steady-state photorefractive solitons (screening solitons [3–4], open- and closed-circuit photovoltaic solitons [5,6], and screening-photovoltaic solitons [7,8]) have been predicted and the first two have been found experimentally [9,10]. At present, the investigations on the PR soliton, soliton pair and soliton interaction were concerned with a single PR crystal [1–17]. Screening solitons are possible in a single biased PR crystal. Can a screening soliton form individually within each crystal in a biased series PR crystal circuit in which two PR crystals, denoted by P and \hat{P} , and a voltage source are connected in a chain by electrode leads (Fig. 1)? That is, when two laser beams are appropriately and, respectively, incident on the two crystals, can a screening soliton form individually within each crystal? If it can, do the two solitons, formed separately in the two crystals, interact or affect each other?

In this paper, we investigate steady-state PR solitons form in a series PR crystal circuit. By use of the well-known transport model of photorefractive effect, successfully used to develop the theories of a screening soliton [4], we predicate that each crystal can support a screening soliton in the case that the spatial extent of the optical wave is much less than

the width of the crystal. We name the two solitons, formed separately in the two crystals, a separate screening soliton pair. Both bright and dark screening solitons can form in the crystals. As a result, there are three types of the separate screening soliton pairs: bright-bright, bright-dark, and dark-dark.

Because the two crystals are connected electronically in such a circuit, when the two crystals are illuminated by two laser beams, the light-induced current in one crystal can flow into the other crystal, and as a result, the bias voltage applied to each crystal will vary with the intensities of two incident laser beams. However, for a single biased PR crystal the bias voltage depends only on the voltage source and does not vary with the intensity of the input laser beam. Therefore, for a biased series PR crystal circuit, changing the intensity of the laser beam incident upon one crystal, not only will the soliton formed in that crystal change, but the soliton formed in the other crystal will also change. That is, the two solitons in a separate screening soliton pair can interact or affect each other by the light-induced current. The interaction is collisionless. Obviously, the interaction will affect the spatial profile, dynamical evolution, stability, and self-deflection of the two solitons in a separate screening soliton pair and the interaction must be different from the interaction between the two solitons in a common soliton pair formed in a single crystal [11–17]. By employing numerical techniques we investigate the effect of the interaction on the spatial profiles, dynamical evolutions, stabilities, and self-deflection of the two solitons in a separate screening soliton pair. Our results show that the two dark solitons in a dark-dark soliton pair can interact with each other by light-induced current, whereas the two bright solitons in a bright-bright soliton pair cannot affect each other by light-induced current. For a dark-bright soliton pair, the dark soliton can affect the bright soliton whereas the bright one cannot affect the dark one by light-induced current, i.e., the interaction is unilateral. In this

*Email address: jsliu4508@sina.com

†Present address: Institute of Applied Physics, Xidian University, Xian 710071, China.

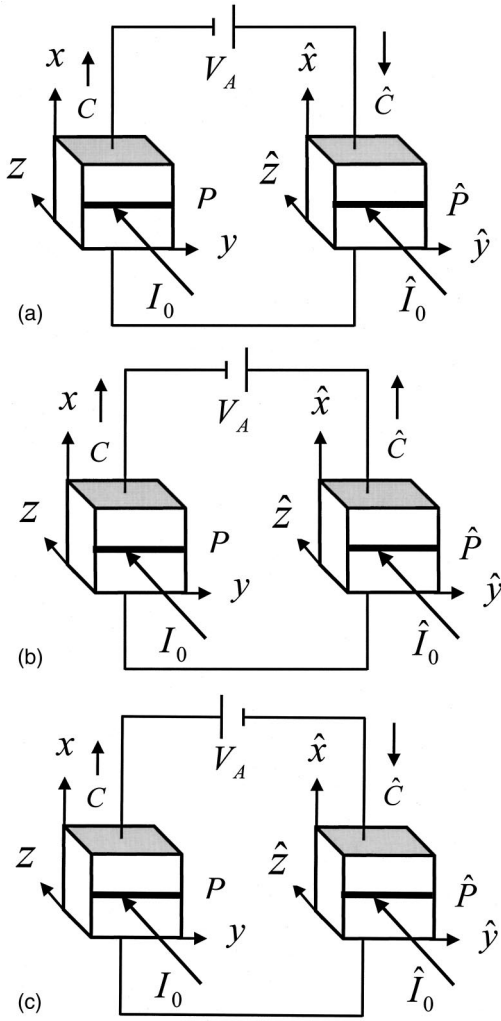


FIG. 1. Illustration of a biased series PR crystal circuit consisting of two PR crystals to support a bright-bright soliton pair in (a), a bright-dark soliton pair in (b), and a dark-dark soliton in (c). P and \hat{P} denote the two crystals, respectively. C and \hat{C} denote the two c axes. I_0 and \hat{I}_0 denote the incident bright or dark solitonlike in one-dimensional laser beams. V_A denotes the voltage of the source.

paper, we only discuss the coupling effects resulting from the light-induced current. The coupling effects resulting from the dark current will be discussed elsewhere.

This paper is organized as follows. In Sec. II, the theoretical model is built upon the well-known transport model of photorefractive effect including the diffusion effects. In Secs. III–V, the coupling effects between the two solitons in a separate screening soliton pair on the intensity profiles, dynamical evolutions, stabilities, and self-deflection of the two solitons are investigated numerically. Finally, we summarize the results, discuss some potential applications, and draw some conclusions in Sec. VI.

II. THEORETICAL MODEL

As shown in Fig. 2, an envisaged experiment is arranged as follows. Two collimated CW laser beams, produced by

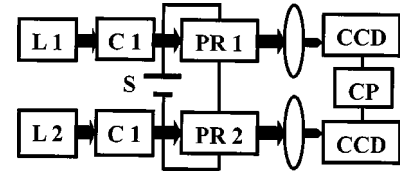


FIG. 2. An envisaged experiment arrangement. $L1$ and $L2$ are the lasers, $C1$ and $C2$ are the collimators, S is the voltage source, $PR1$ and $PR2$ are the PR crystals, and CP is a computer.

two separate lasers, are adjusted into bright or dark one-dimensional solitonlike beams and then imaged onto the front surfaces of the two crystals, respectively. For each crystal, electrodes are made on the two surfaces with their normal parallel to the c axis of the crystal. Electrode leads connect the two crystals electronically in a chain with a voltage source. Each crystal is oriented with its c axis perpendicular to the direction of the laser beam. The beam profiles can be detected by two charged coupled device (CCD) arrays respectively. In general, the crystals P and \hat{P} are different types of PR crystal; P is a SBN crystal and \hat{P} is a TaBiO₃ crystal. Therefore, the two crystals in Figs. 1(a) and 1(c) differ from one large crystal.

A. The expression of space-charge field

Considering first the crystal P , an optical beam propagates in the crystal along the z axis and is permitted to diffract only along the x direction. The crystal's optical c axis orients along the x coordinate. Moreover, let us assume that the optical beam is linearly polarized along the x direction and the bias voltage is applied along the same direction. Under these conditions the perturbed extraordinary refractive index \bar{n}_e (along the c axis) is given by $(\bar{n}_e)^2 = n_e^2 - n_e^4 r_{33} E_{SC}$, where r_{33} is the electro-optic coefficient, n_e is the unperturbed extraordinary index of refraction, and E_{SC} is the induced space-charge field. On the other hand, the electric-field component \mathbf{E} of the optical beam satisfies the Helmholtz equation

$$\nabla^2 \mathbf{E} + (k_0 \bar{n}_e)^2 \mathbf{E} = 0, \quad (1)$$

where $k_0 = 2\pi/\lambda_0$ and λ_0 is the free-space wavelength of the lightwave employed. By expressing \mathbf{E} in terms of a slowly varying envelope ϕ , i.e., $\mathbf{E} = \hat{x} \phi(x, z) \exp(ikz)$, where $k = k_0 n_e$, one can find that Eq. (1) leads to the following paraxial equation of diffraction:

$$i \frac{\partial \phi}{\partial z} + \frac{1}{2k} \frac{\partial^2 \phi}{\partial x^2} - \frac{k_0}{2} (n_e^3 r_{33} E_{SC}) \phi = 0. \quad (2)$$

To simplify the analysis, we have neglected any loss effects in Eq. (2).

In turn, the induced space-charge field E_{SC} can be obtained from the standard set of rate and continuity equations and Gauss's law, which describe the photorefractive effect in a medium. In the steady state, the one-dimensional equations are [4]

$$\gamma_R n N_D^+ = s_i (I + I_d) (N_D - N_D^+), \quad (3)$$

$$\frac{\partial E_{SC}}{\partial x} = \frac{e}{\epsilon_0 \epsilon_r} (N_D^+ - N_A - n), \quad (4)$$

$$J = e \mu n E_{SC} + k_B T \mu \frac{\partial n}{\partial x}, \quad (5)$$

$$\frac{\partial J}{\partial x} = 0 \quad \text{or} \quad J = \text{const}, \quad (6)$$

where N_D^+ and N_D are the ionized donor density and donor density, respectively, N_A is the acceptor density, n is the electron density, J is the current density, s_i is the photoexcitation cross section, γ_R is the carrier recombination rate, μ and e are, respectively, the electron mobility and the charge, k_B is Boltzmann's constant, T is the absolute temperature, ϵ_r is the relative static dielectric constant, and I_d is the so-called dark irradiance. $I = I(x, z)$ is the power density profile of the optical beam, which can be also expressed in terms of the envelope ϕ by use of Poynting's theorem, i.e., $I = (n_e/2\eta_0)|\phi|^2$, where $\eta_0 = (\mu_0/\epsilon_0)^{1/2}$. Moreover, in Eqs. (3)–(6) we have ignored any z spatial dependence by assuming that the variables involved vary much more rapidly in the x direction.

Even though the expression for E_{SC} can be obtained in principle from Eqs. (3)–(6), this task is considerably involved. However, we follow Ref. [4] to greatly simplify Eqs. (3)–(6) by keeping in mind that the following inequalities hold true in typical PR media: $N_D^+ \gg n$, $N_D \gg n$, and $N_A \gg n$. In this case, Eqs. (3) and (4) yield the following results:

$$N_D^+ = N_A \left(1 + \frac{\epsilon_0 \epsilon_r}{e N_A} \frac{\partial E_{SC}}{\partial x} \right), \quad (7)$$

$$n = \frac{s_i (N_D - N_A)}{\gamma_R N_A} (I + I_d) \left(1 + \frac{\epsilon_0 \epsilon_r}{e N_A} \frac{\partial E_{SC}}{\partial x} \right)^{-1}. \quad (8)$$

Furthermore, if $I(x, z)$ varies slowly with respect to x , then in typical PR media the dimensionless term $[(\epsilon_0 \epsilon_r / e N_A)(\partial E_{SC} / \partial x)]$ is expected to be much less than unity [4]. Under this condition, Eqs. (7) and (8) yield the following results:

$$N_D^+ = N_A, \quad (9)$$

$$n = \frac{s_i (N_D - N_A)}{\gamma_R N_A} (I + I_d). \quad (10)$$

At this point, let us also assume that $I = I(x, z)$ attains asymptotically a constant value at $x \rightarrow \pm\infty$, i.e., $I(x \rightarrow \pm\infty, z) = I_\infty$. In these regions of constant illumination, Eqs. (3)–(6) require that E_{SC} is independent of x , i.e., $E_{SC}(x \rightarrow \pm\infty, z) = E_0$, where E_0 is the external bias field. Therefore, from Eq. (8) the electron density n in the regions ($x \rightarrow \pm\infty$), denoted by n_∞ , can be subsequently determined and is given by

$$n_\infty = s_i (N_D - N_A) (I_\infty + I_d) / (\gamma_R N_A). \quad (11)$$

On the other hand, from Eq. (5), the current density J in the regions ($x \rightarrow \pm\infty$), denoted by $J_\infty = J(x \rightarrow \pm\infty, z)$, can be given by

$$J_\infty = e \mu n_\infty E_0. \quad (12)$$

For the crystal \hat{P} , we likewise have

$$\hat{n}_\infty = \hat{s}_i (\hat{N}_D - \hat{N}_A) (\hat{I}_\infty + \hat{I}_d) / (\hat{\gamma}_R \hat{N}_A), \quad (13)$$

$$\hat{J}_\infty = e \hat{\mu} \hat{n}_\infty \hat{E}_0. \quad (14)$$

Let V_A denote the voltage of the source. Let V and \hat{V} denote the potential measured between the electrodes of the P and \hat{P} crystals having width separated by W and \hat{W} , respectively. Let S and \hat{S} denote the surfaces of the electrodes of the crystals P and \hat{P} , respectively. In the series circuit, we have $V_A = V + \hat{V}$ and $SJ = \hat{S}\hat{J}$. If the spatial extent Δx of the optical wave is much less than the x width W of the crystal, E_0 is approximately expressed by $E_0 = V/W$ [4]. For the crystal \hat{P} , we likewise have $\hat{E}_0 = \hat{V}/\hat{W}$. Obviously, we find that

$$V_A = WE_0 + \hat{W}\hat{E}_0. \quad (15)$$

Equation (6) implies that J is constant everywhere in the crystal, that is, $J(x, z) = J_\infty$. For the crystal \hat{P} , we likewise have $\hat{J}_\infty = \hat{J}(x, z)$. As a result, we find that

$$SJ_\infty = \hat{S}\hat{J}_\infty. \quad (16)$$

Substitution of Eqs. (12) and (14) into Eq. (16), we find that

$$S\mu n_\infty E_0 = \hat{S}\hat{\mu} \hat{n}_\infty \hat{E}_0. \quad (17)$$

From Eqs. (15) and (17), we determine that

$$E_0 = g E_A, \quad (18)$$

$$\hat{E}_0 = \hat{g} \hat{E}_A, \quad (19)$$

$$g = \hat{\delta} (\hat{I}_\infty + \hat{I}_d) / [\delta (I_\infty + I_d) + \hat{\delta} (\hat{I}_\infty + \hat{I}_d)], \quad (20)$$

$$\hat{g} = \delta (I_\infty + I_d) / [\delta (I_\infty + I_d) + \hat{\delta} (\hat{I}_\infty + \hat{I}_d)], \quad (21)$$

where $\delta = S\mu s_i (N_D - N_A) / (r_R N_A W)$, $E_A = V_A / W$, $\hat{\delta} = \hat{S}\hat{\mu}\hat{s}_i (\hat{N}_D - \hat{N}_A) / (\hat{r}_R \hat{N}_A \hat{W})$, and $\hat{E}_A = V_A / \hat{W}$. The parameters g and \hat{g} are known as coupling coefficients between the two solitons and $g + \hat{g} = 1$.

In the region of $I(x, z)$ varying with x , from Eqs. (3) and (5), we have

$$J = e \mu n \left(E_{SC} + \frac{K_B T}{e} \frac{\partial \ln n}{\partial x} \right). \quad (22)$$

From $J(x, z) = J_\infty$ and Eqs. (12) and (22), we have

$$n \left(E_{\text{SC}} + \frac{K_B T}{e} \frac{\partial \ln n}{\partial x} \right) = n_{\infty} E_0. \quad (23)$$

In turn, the expression for E_{SC} can be obtained from Eq. (23) as follows:

$$E_{\text{SC}} = g E_A \frac{I_{\infty} + I_d}{I + I_d} - \frac{K_B T}{e} \frac{1}{I + I_d} \frac{\partial I}{\partial x}. \quad (24)$$

Similarly, we can obtain results for \hat{P} as follows:

$$\hat{E}_{\text{SC}} = \hat{g} \hat{E}_A \frac{\hat{I}_{\infty} + \hat{I}_d}{\hat{I} + \hat{I}_d} - \frac{K_B \hat{T}}{e} \frac{1}{\hat{I} + \hat{I}_d} \frac{\partial \hat{I}}{\partial \hat{x}}. \quad (25)$$

Although the expression for E_{SC} (as well as \hat{E}_{SC}) has a similar form to that for the space-charge field in a single biased photorefractive crystal [4], the value of E_{SC} (as well as \hat{E}_{SC}) depends on the parameters of the two crystals, including I_{∞} and \hat{I}_{∞} . On the other hand, E_{SC} and \hat{E}_{SC} are not independent. They couple each other by the coupling coefficients g and \hat{g} .

B. Envelope evolution equation

Considering first the crystal P , the envelope evolution equation can now be established by insertion of Eq. (24) into Eq. (2). It proves more convenient, however, to study this equation in a normalized fashion. To do so, let us adopt the following dimensionless coordinates and variables: i.e., let $\xi = z/(kx_0^2)$, $s = x/x_0$, and $\phi = (2\eta_0 I_d/n_e)^{1/2} U$. Here x_0 is an arbitrary spatial width. Using Eqs. (2) and (24), we can then show that the normalized envelope U obeys the following dynamical evolution equation:

$$iU_{\xi} + \frac{1}{2} U_{ss} - \beta(\rho + 1) \frac{U}{1 + |U|^2} + \gamma \frac{(|U|^2)_s U}{1 + |U|^2} = 0, \quad (26)$$

where $\rho = I_{\infty}/I_d$, $\beta = g\sigma E_A$, $\gamma = \sigma K_B T/(x_0 e)$, and $\sigma = (k_0 x_0)^2 (\hat{n}_e^4 r_{33}/2)$.

Similarly, we can obtain results for \hat{P} as follows:

$$i\hat{U}_{\xi} + \frac{1}{2} \hat{U}_{\hat{s}\hat{s}} - \hat{\beta}(\hat{\rho} + 1) \frac{\hat{U}}{1 + |\hat{U}|^2} + \hat{\gamma} \frac{(|\hat{U}|^2)_{\hat{s}} \hat{U}}{1 + |\hat{U}|^2} = 0, \quad (27)$$

where $\hat{\rho} = \hat{I}_{\infty}/\hat{I}_d$, $\hat{\beta} = \hat{g}\hat{\sigma}\hat{E}_A$, $\hat{\gamma} = \hat{\sigma}K_B\hat{T}/(\hat{x}_0 e)$, $\hat{\sigma} = (k_0 \hat{x}_0)^2 (\hat{n}_e^4 \hat{r}_{33}/2)$, $\hat{\xi} = \hat{z}/(k\hat{x}_0^2)$, and $\hat{s} = \hat{x}/\hat{x}_0$. Although the two dynamical evolution equations have a similar form to that for a single biased photorefractive crystal [4], they couple each other by the coupling coefficients g and \hat{g} .

C. Dark-dark screening soliton pair

We begin our analysis by considering a dark-dark screening soliton pair, i.e., both crystals support dark screening soliton. First, this dark soliton solution in the crystal P can be derived from Eq. (26) by expressing the beam envelope U in the usual fashion: $U = \rho^{1/2} y(s) \exp(i\nu\xi)$, where ν represents a nonlinear shift of the propagation constant and $y(s)$ is a

normalized real function bounded between $0 \leq y(s) \leq 1$ and denotes the normalized field profile. For the dark spatial solitons, we require that $y(0) = 0$, $y(\infty) = 0$, and $y(s \rightarrow \pm\infty) = 1$. Substitution of this latter form of U into Eq. (26) (with $\gamma = 0$) yields

$$\frac{d^2 y}{ds^2} - 2\nu y - 2\beta(\rho + 1) \frac{y}{1 + \rho y^2} = 0, \quad (28)$$

from which one can readily deduce that $\nu = -\beta$ and

$$\left(\frac{dy}{ds} \right)^2 = -2\beta \left[(y^2 - 1) - \frac{\rho + 1}{\rho} \ln \left(\frac{1 + \rho y^2}{1 + \rho} \right) \right]. \quad (29)$$

For integration of Eq. (29), the normalized dark-field profile $y(s)$ can be determined from the following equation:

$$(-2\beta)^{1/2} s = \pm \int_{y(s)}^0 \frac{d\bar{y}}{\left[(\bar{y}^2 - 1) - \frac{\rho + 1}{\rho} \ln \left(\frac{1 + \rho \bar{y}^2}{1 + \rho} \right) \right]^{1/2}}. \quad (30)$$

Similarly, for the crystal \hat{P} , we have $\hat{U} = \hat{\rho}^{1/2} \hat{y}(\hat{s}) \exp(i\hat{\nu}\hat{\xi})$, $\hat{\nu} = -\hat{\beta}$, and

$$\left(\frac{d\hat{y}}{d\hat{s}} \right)^2 = -2\hat{\beta} \left[(\hat{y}^2 - 1) - \frac{\hat{\rho} + 1}{\hat{\rho}} \ln \left(\frac{1 + \hat{\rho} \hat{y}^2}{1 + \hat{\rho}} \right) \right], \quad (31)$$

$$(-2\hat{\beta})^{1/2} \hat{s} = \pm \int_{\hat{y}(\hat{s})}^0 \frac{d\bar{\hat{y}}}{\left[(\bar{\hat{y}}^2 - 1) - \frac{\hat{\rho} + 1}{\hat{\rho}} \ln \left(\frac{1 + \hat{\rho} \bar{\hat{y}}^2}{1 + \hat{\rho}} \right) \right]^{1/2}}. \quad (32)$$

Equations (29) and (31), or (30) and (32) predict that a dark-dark screening soliton pair can exist in a biased series PR crystal circuit. The conditions necessary for a dark-dark soliton pair in the crystals P and \hat{P} are $E_A < 0$ and $\hat{E}_A < 0$, which can be realized by appropriately orienting the c axes of the two crystals and the polarity of the external bias field.

D. Bright-dark soliton pair

For a bright-dark soliton pair, let us assume that the bright soliton forms in the crystal P and the dark one forms in the crystal \hat{P} . For the bright soliton, the optical beam intensity is expected to vanish at infinity ($s \rightarrow \pm\infty$), i.e., $I_{\infty} = 0$ and then $\rho = I_{\infty}/I_d = 0$. From Eq. (26), bright-type waves should therefore satisfy

$$iU_{\xi} + \frac{1}{2} U_{ss} - \beta \frac{U}{1 + |U|^2} + \gamma \frac{(|U|^2)_s U}{1 + |U|^2} = 0. \quad (33)$$

By entirely neglecting the effect of diffusion, bright soliton solutions can be derived from Eq. (33) by expressing the beam envelope U in the usual fashion: $U = r^{1/2} y(s) \exp(i\nu\xi)$. The positive quantity r is defined as $r = I_0/I_d = I(0,0)/I_d$. For the bright spatial solitons, we require that $y(0) = 1$, $y(\infty) = 0$, and $y(s \rightarrow \pm\infty) = 0$. Substitution of this latter form of U into Eq. (33) (with $\gamma = 0$) yields

$$\frac{d^2y}{ds^2} - 2\nu y - 2\beta \frac{y}{1+ry^2} = 0. \quad (34)$$

By integrating Eq. (34) once and by employing the y -boundary conditions, we find that

$$\nu = -(\beta/r)\ln(1+r), \quad (35)$$

$$\left(\frac{dy}{ds}\right)^2 = \frac{2\beta}{r} [\ln(1+ry^2) - y^2 \ln(1+r)]. \quad (36)$$

Further integration of Eq. (36) leads

$$(2\beta)^{1/2}s = \pm \int_{y(s)}^1 \frac{r^{1/2}d\bar{y}}{[\ln(1+r\bar{y}^2) - \bar{y}^2 \ln(1+r)]^{1/2}}. \quad (37)$$

The dark soliton profiles in the bright-dark soliton pair can be obtained by use of a similar way to above and determined by the following equation:

$$(-2\hat{\beta})^{1/2} = \pm \int_{\hat{y}(\hat{s})}^0 \frac{d\bar{y}}{\left[(\bar{y}^2 - 1) - \frac{1+\hat{\rho}}{\hat{\rho}} \ln\left(\frac{1+\hat{\rho}\bar{y}^2}{1+\hat{\rho}}\right) \right]^{1/2}}. \quad (38)$$

Equations (37) and (38) predict that a bright-dark screening soliton pair can exist in a biased series PR crystal circuit. The conditions necessary for a bright-dark soliton pair in the crystals P and \hat{P} are $E_A > 0$ and $\hat{E}_A < 0$.

E. Bright-bright soliton pair

Now let us consider a bright-bright soliton pair. The bright soliton profiles in a bright-bright soliton pair can be obtained by use of a similar way to above and determined by the following equations:

$$(2\beta)^{1/2}s = \pm \int_{y(s)}^1 \frac{r^{1/2}d\bar{y}}{[\ln(1+r\bar{y}^2) - \bar{y}^2 \ln(1+r)]^{1/2}}, \quad (39)$$

$$(2\hat{\beta})^{1/2}\hat{s} = \pm \int_{\hat{y}(\hat{s})}^1 \frac{\hat{r}^{1/2}d\bar{y}}{[\ln(1+\hat{r}\bar{y}^2) - \bar{y}^2 \ln(1+\hat{r})]^{1/2}}, \quad (40)$$

$$\nu = -(\beta/r)\ln(1+r) \text{ and } \hat{\nu} = -(\hat{\beta}/\hat{r})\ln(1+\hat{r}).$$

Equations (39) and (40) predict that a bright-bright screening soliton pair can exist in a biased series PR crystal circuit. The conditions necessary for a bright-bright soliton pair in the crystals P and \hat{P} are $E_A > 0$ and $\hat{E}_A > 0$.

III. SPATIAL PROFILES OF SEPARATE SCREENING SOLITON PAIRS AND COUPLING EFFECTS

A. Coupling effects

Let us consider the coupling effects between the two solitons in a separate screening soliton pair. In a biased series PR crystal circuit, two crystals are connected electronically. When optical beams illuminate on the crystals, the light-induced current will flow from one crystal to another. As a result, the two solitons, supported separately by the two crystals,

will affect each other. Because g and \hat{g} depend on the parameters of the two crystals, the character of the soliton in one crystal not only depends on the parameters of that crystal, but also depends on the parameters of the other crystal. In other words, the character of any soliton in a soliton pair depends on the parameters of the two crystals.

For a biased series PR crystal circuit, when the input intensity of one crystal changes, not only will the soliton in that crystal change, but also the soliton in the other crystal will change. For a dark-dark screening soliton pair, we have $I_\infty \neq 0$ and $\hat{I}_\infty \neq 0$. Because g and \hat{g} depend on I_∞ and \hat{I}_∞ , changing the input intensity of a dark soliton can affect the other dark soliton. In other words, the two dark soliton can interact each other by the light-induced current that flows from one crystal to another. The interaction is collisionless or contactless optically. However, for a bright-dark screening soliton pair, we have $I_\infty = 0$ and $\hat{I}_\infty \neq 0$. As a result, g and \hat{g} are independent of I_∞ . Interestingly, this result brings on the dark soliton can affect the bright one by the light-induced current, but the bright soliton cannot affect the dark one. That is, changing the input intensity of the dark soliton can affect the bright one whereas changing the input intensity of the bright soliton cannot affect the dark one. The unilateral effect may be useful in some applications. Furthermore, for a bright-bright soliton pair, because $I_\infty = 0$ and $\hat{I}_\infty = 0$ and g and \hat{g} are independent of I_∞ and \hat{I}_∞ . Therefore, the two bright solitons cannot affect each other by the light-induced current. That is, changing the input intensity of a bright soliton cannot affect the other bright soliton.

Noteworthy, the above results are obtained under the limit of the spatial extent Δx ($\Delta \hat{x}$) of the optical wave being much less than the x (\hat{x}) width W (\hat{W}) of the crystal P (\hat{P}). In fact, in this limit, when a crystal supports a bright soliton, the light-induced current is so small that it can be neglected, whereas when a crystal supports a dark soliton the light-induced current is big enough. Taking an example, for a photovoltaic crystal, $J \propto W/\Delta x \gg 1$ for a dark soliton whereas $J \propto \Delta x/W \ll 1$ for a bright soliton [6]. As a result, in the limit of $\Delta x/W \ll 1$, when a crystal supports a bright soliton, the light-induced current is too weak to affect the other soliton, whereas when a crystal supports a dark soliton, the light-induced current is strong enough to affect the other soliton in the other crystal. Of course, when the condition of $\Delta x/W \ll 1$ is not satisfied, we should reconsider these problems. When the light-induced current from a bright soliton cannot be neglected, the bright soliton maybe affect the other soliton in the separate screening soliton pair.

It is important to note that for bright-bright screening solitons, $I_\infty = 0$ and $\hat{I}_\infty = 0$, from Eqs. (20) and (21), we know that the coupling effects between the two bright solitons will result from the dark irradiances. Of course, the coupling effects resulting from the dark irradiances not only can occur in a bright-bright soliton pair, but also can occur in a dark-dark and a bright-dark soliton pairs and, when $I_\infty \ll I_d$ and $\hat{I}_\infty \ll \hat{I}_d$, the dark irradiances will play a key role in the coupling effects. To be limited by the space, the coupling effects

resulting from the dark irradiances will be discussed elsewhere.

B. Dark-dark screening soliton pairs

Let us consider the effects of the interaction between the two solitons in a separate screening soliton pair on the intensity profilers of the two solitons. In order to provide some relevant examples, two SBN (strontium barium niobate) crystals are taken as P and \hat{P} . The two crystals have the following parameters: $\gamma_{33} = \hat{\gamma}_{33} = 237 \times 10^{-12}$ m/V, $n_e = \hat{n}_e = 2.33$, $W = \hat{W} = 1$ cm, $S = \hat{S}$, $\delta = \hat{\delta}$, and $I_d = \hat{I}_d$. The arbitrary scales are $x_0 = \hat{x}_0 = 40$ μm and the wavelengths are $\lambda_0 = \hat{\lambda}_0 = 0.5$ μm . For this set of values, we have $\sigma = \hat{\sigma} = 88.24 \times 10^{-5}$ m/V. The voltage of the source is $V_A = 100$ V.

First, let us consider the case of a dark-dark screening soliton pair formed in the configuration shown in Fig. 1(c). In this configuration, we have $E_A = \hat{E}_A = -10^4$ V/m. In the first place, we take $\rho = I_\infty/I_d = 1$ and $\hat{\rho} = \hat{I}_\infty/\hat{I}_d = 1$. From Eqs. (20) and (21), we find that $g = \hat{g} = 1/2$. From $\beta = g\sigma E_A$ and $\hat{\beta} = \hat{g}\hat{\sigma}\hat{E}_A$ we have $\beta = \hat{\beta} = -4.41$. With these values, the normalized intensity profiles of the two dark solitons in the crystals P and \hat{P} , denoted by $y^2(s)$ and $\hat{y}^2(\hat{s})$, are obtained by solving Eqs. (30) and (32), as shown in Fig. 3(a) curve 1 and 3(b) curve 1, respectively. When the input intensity of the crystal P increases but the other parameters remain unchanged, such as ρ increases from 1 to 10, not only does the dark soliton in the crystal P change as shown in Fig. 3(a) curve 2, but also the dark soliton in crystal \hat{P} changes as shown in Fig. 3(b) curve 2. The two curves are calculated at $I_\infty = 10I_d$, $\rho = 10$, $g = \frac{2}{13}$, $\beta = -1.36$ and $\hat{I}_\infty = \hat{I}_d$, $\hat{\rho} = 1$, $\hat{g} = \frac{11}{13}$, $\hat{\beta} = -7.48$. From this set of values we can see that, for a separate dark-dark screening soliton pair, the dark soliton in a strong input intensity can be obtained for a smaller nonlinearity than for a weaker input intensity. By the same token, when the input intensity of the crystal \hat{P} increases but the other parameters remain unchanged, such as $\hat{\rho}$ increases from 1 to 20, not only does the dark soliton in crystal \hat{P} change as shown in Fig. 3(b) curve 3, but also the dark soliton in the crystal P changes as shown in Fig. 3(a) curve 3. The two curves are calculated at $I_\infty = I_d$, $\rho = 1$, $g = \frac{21}{23}$, $\beta = -8.07$ and $\hat{I}_\infty = 20\hat{I}_d$, $\hat{\rho} = 20$, $\hat{g} = \frac{2}{23}$, $\hat{\beta} = -0.77$. The above results imply that, for a dark-dark soliton pair, a dark soliton can affect the profile of the other dark soliton by the light-induced current. In other words, the two dark solitons in a dark-dark soliton pair can interact each other.

C. Bright-dark screening soliton pairs

Then, let us consider the case of a bright-dark screening soliton pair formed in the configuration shown in Fig. 1(b). In the configuration, we have $E_A = 10^4$ V/m and $\hat{E}_A = -10^4$ V/m. If we assume that the crystal P supports a bright soliton, we have $\rho = I_\infty/I_d = 0$. In the first place, we take $r = I_0/I_d = 1$ and $\hat{\rho} = \hat{I}_\infty/\hat{I}_d = 1$. From Eqs. (20) and (21) as

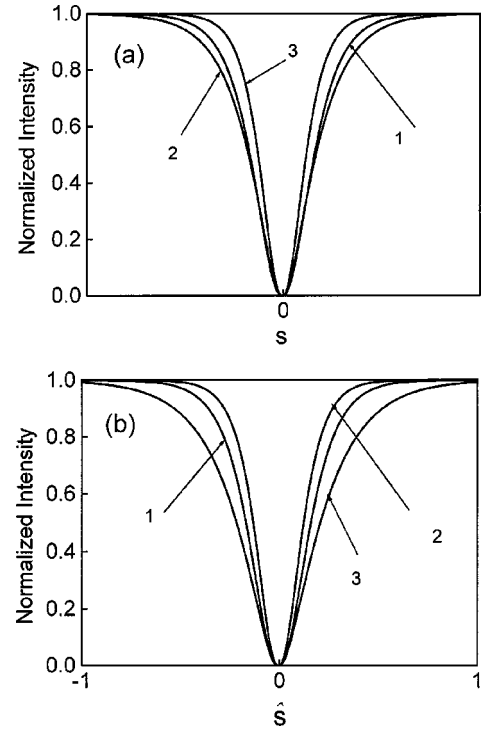


FIG. 3. Dark-dark separate screening soliton pairs in a biased series SBN crystal circuit. (a) Dark soliton profiles in the crystal P . (b) Dark soliton profiles in the crystal \hat{P} .

well as $\beta = g\sigma E_A$ and $\hat{\beta} = \hat{g}\hat{\sigma}\hat{E}_A$, we find that $g = \frac{2}{3}$, $\hat{g} = \frac{1}{3}$, $\beta = 5.9$, and $\hat{\beta} = -2.95$. With these values, the normalized intensity profiles of the bright soliton in the crystal P , denoted by $y^2(s)$, and the dark soliton in the crystal \hat{P} , denoted by $\hat{y}^2(\hat{s})$, are obtained by solving Eqs. (37) and (38), as shown in Fig. 4(a) curve 1 and Fig. 4(b) curve 1, respectively. When the input intensity of the crystal \hat{P} increases but the other parameters remain unchanged, such as $\hat{\rho}$ increases from 1 to 50, not only does the dark soliton in the crystal \hat{P} change as shown in Fig. 4(b) curve 2, but also the bright soliton in the crystal P changes as shown in Fig. 4(a) curve 2. The two curves are calculated at $I_\infty = 0$, $I_0 = I_d$, $r = 1$, $g = \frac{51}{52}$, $\beta = 8.67$ and $\hat{I}_\infty = 50\hat{I}_d$, $\hat{\rho} = 50$, $\hat{g} = \frac{1}{52}$, $\hat{\beta} = -0.17$. From this set of values we can see that for a separate bright-dark screening soliton pair, the dark soliton in a strong input intensity can be obtained for a smaller nonlinearity than for a weaker input intensity. It should be noted that when the input intensity of the crystal P increases but the other parameters remain unchanged, such as r increases from 1 to 50 but $\hat{\rho}$ keeps $\hat{\rho} = 1$, only the bright soliton in the crystal P changes as shown in Fig. 4(a) curve 3, but the dark soliton in the crystal \hat{P} does not change as shown in Fig. 4(b) curve 3. The two curves are calculated at $I_\infty = 0$, $r = 50$, $g = \frac{2}{3}$, $\beta = 5.9$ and $\hat{I}_\infty = \hat{I}_d$, $\hat{\rho} = 1$, $\hat{g} = \frac{1}{3}$, $\hat{\beta} = -2.95$. The above results imply that, for a bright-dark soliton pair, the dark soliton can affect the profile of the bright soliton by the light-induced current, whereas the bright soliton cannot affect the profile of the dark soliton.

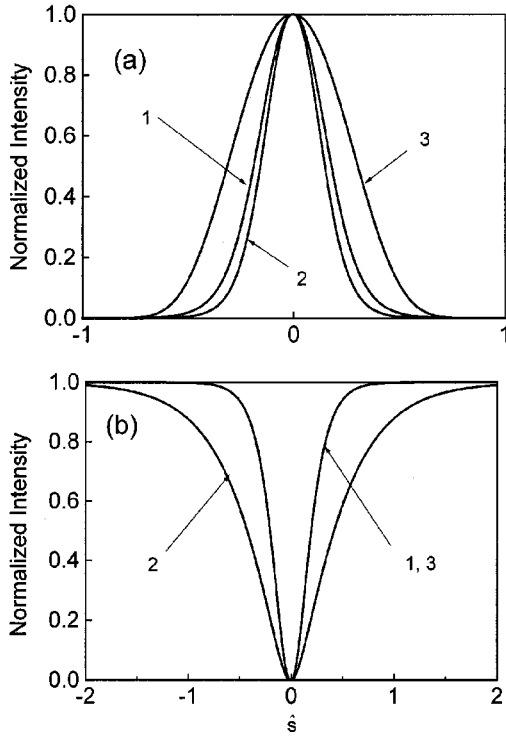


FIG. 4. Bright-dark separate screening soliton pairs in a biased series SBN crystal circuit. (a) Bright soliton profiles in the crystal P . (b) Dark soliton profiles in the crystal \hat{P} .

D. Bright-bright screening soliton pairs

Last, let us consider the case of a bright-bright soliton pair formed in the configuration shown in Fig. 1(a). In this configuration, we have $E_A = \hat{E}_A = 10^4$ V/m. For the two bright solitons, we have $I_\infty = 0$ and $\hat{I}_\infty = 0$. From Eqs. (20) and (21) as well as $\beta = g\sigma E_A$ and $\hat{\beta} = \hat{g}\hat{\sigma}\hat{E}_A$, we have $g = \hat{g} = \frac{1}{2}$ and $\beta = \hat{\beta} = 4.41$ for any values of r and \hat{r} . In the first place, we take $r = I_0/I_d = 1$ and $\hat{r} = \hat{I}_0/\hat{I}_d = 1$. With these values, the normalized intensity profiles of the two bright solitons in the crystals P and \hat{P} , denoted by $y^2(s)$ and $\hat{y}^2(\hat{s})$, are obtained by solving Eqs. (39) and (40), as shown in Figs. 5(a) curve 1 and 5(b) curve 1, respectively. When the input intensity of the crystal P increases but the other parameters remain unchanged, such as r increases from 1 to 50, only the bright soliton in the crystal P changes as shown in Fig. 5(a) curve 2, but the other bright soliton in the crystal \hat{P} does not change as shown in Fig. 5(b) curve 2. The two curves are calculated at $r = 50$, $g = \frac{1}{2}$, $\beta = 4.41$ and $\hat{r} = 1$, $\hat{g} = \frac{1}{2}$, $\hat{\beta} = 4.41$. By the same token, when the input intensity of the crystal \hat{P} increases but the other parameters remain unchanged, such as \hat{r} increases from 1 to 50, only the bright soliton in the crystal \hat{P} changes, as shown in Fig. 5(b) curve 3, but the other bright soliton in the crystal P does not change, as shown in Fig. 5(a) curve 3. The two curves are calculated at $r = 1$, $g = \frac{1}{2}$, $\beta = 4.41$ and $\hat{r} = 50$, $\hat{g} = \frac{1}{2}$, $\hat{\beta} = 4.41$. Above results imply that for a bright-bright screening soliton pair, the two bright solitons cannot affect each other by the light-induced current. However, for a bright-bright

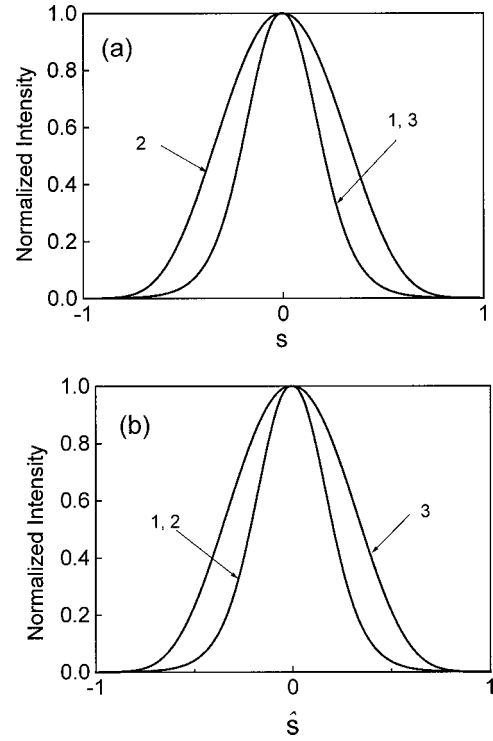


FIG. 5. Bright-bright separate screening soliton pairs in a biased series SBN crystal circuit. (a) Bright soliton profiles in the crystal P . (b) Bright soliton profiles in the crystal \hat{P} .

soliton pair, the dark irradiances will play a key role in the coupling effects between the two bright solitons. To be limited by the space, the coupling effects resulting from the dark irradiances will be discussed somewhere.

IV. DYNAMICAL EVOLUTIONS OF OPTICAL BEAMS IN A BIASED SERIES PR CRYSTAL CIRCUIT AND COUPLING EFFECTS

Let us consider that two bright or dark solitonlike beams are incident upon the two crystals, respectively, in a biased series SBN crystal circuit as shown in Fig. 1. The coupling effects between the two beams on the dynamical evolutions of the two beams in the circuit can be investigated by numerically solving Eqs. (26) and (27) under appropriate conditions. In this section, we neglect the effects of diffusion process. To do so, we should take $\gamma = \hat{\gamma} = 0$ in Eqs. (26) and (27).

A. Dark-dark screening soliton pairs

Let us consider that two dark solitary beams evolve in a biased series SBN crystal circuit as shown in Fig. 1(c) with $E_A = \hat{E}_A = -10^4$ V/m. The circuit has the same parameters as above. First, we consider the evolutions of two previously found solitary states as the incident beams with the input intensities $\rho = I_\infty/I_d = 1$ and $\hat{\rho} = \hat{I}_\infty/\hat{I}_d = 1$, respectively. From Eqs. (20) and (21) as well as $\beta = g\sigma E_A$ and $\hat{\beta} = \hat{g}\hat{\sigma}\hat{E}_A$, we have $g = \hat{g} = \frac{1}{2}$ and $\beta = \hat{\beta} = -4.44$. The field profiles of the two dark solitary states, denoted by $y_0(s)$ and $\hat{y}_0(\hat{s})$, can be

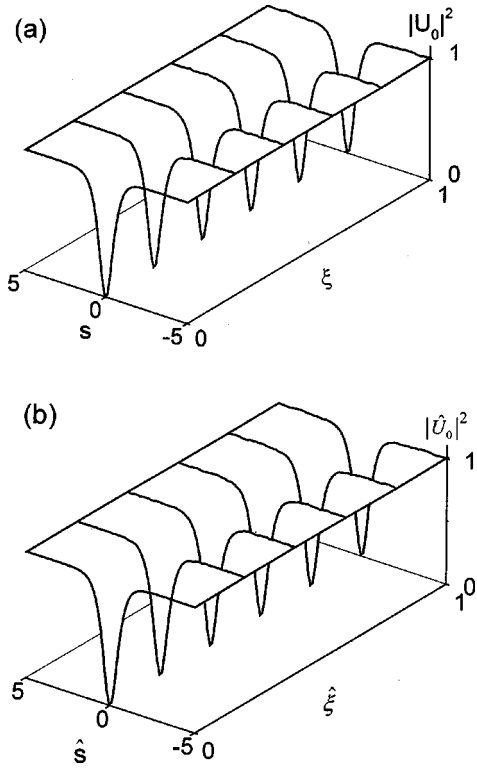


FIG. 6. Dynamical evolutions of the two dark solitary states U_0 and \hat{U}_0 in a biased series SBN crystal circuit. (a) U_0 in the crystal P and (b) \hat{U}_0 in the crystal \hat{P} .

determined by solving Eq. (30) with $\beta = -4.44$ and $\rho = 1$ as well as Eq. (32) with $\hat{\beta} = -4.44$ and $\hat{\rho} = 1$, respectively. We then get the two dark solitary states $U_0 = \sqrt{1}y_0(s)$ and $\hat{U}_0 = \sqrt{1}\hat{y}_0(\hat{s})$. Taking the two solitary states as input beams, their evolutions in the circuit are investigated by numerically solving Eqs. (26) and (27) with $\beta = \hat{\beta} = -4.44$ and $\rho = \hat{\rho} = 1$. As expected, our results confirm that the two dark soliton states remain invariant with propagation distance as shown in Fig. 6.

We then consider the stabilities and the coupling effects between two dark solitary beams in the circuit. To do so, we follow the evolution of an optical beam in the crystal P with an incident beam U_1 whose field profile is still $y_0(s)$, but its maximum amplitude is $\sqrt{10}$, i.e., $U_1 = \sqrt{10}y_0(s)$ and, simultaneously, we observe the evolution of $\hat{U}_0 = \sqrt{1}\hat{y}_0(\hat{s})$ in the crystal \hat{P} . Noteworthily, U_1 is not a solitary state supported by the crystal P , whereas \hat{U}_0 is still a solitary state supported by the crystal \hat{P} . For this case, we have $\rho = I_\infty/I_d = 10$, $\hat{\rho} = \hat{I}_\infty/\hat{I}_d = 1$, $g = \frac{2}{13}$, $\hat{g} = \frac{1}{13}$, $\beta = -1.37$, and $\hat{\beta} = -7.51$. The evolutions of U_1 and \hat{U}_0 are investigated by numerically solving Eq. (26) with $\beta = -1.37$ and $\rho = 10$ as well as Eq. (27) with $\hat{\beta} = -7.51$ and $\hat{\rho} = 1$, respectively, as shown in Fig. 7. As we can see, U_1 reshapes itself and tries to evolve into a solitary wave after a short distance, whereas \hat{U}_0 cannot remain invariant with propagation distance and tries to evolve into a different solitary wave after a short distance. When the maximum amplitude of the input beam for the

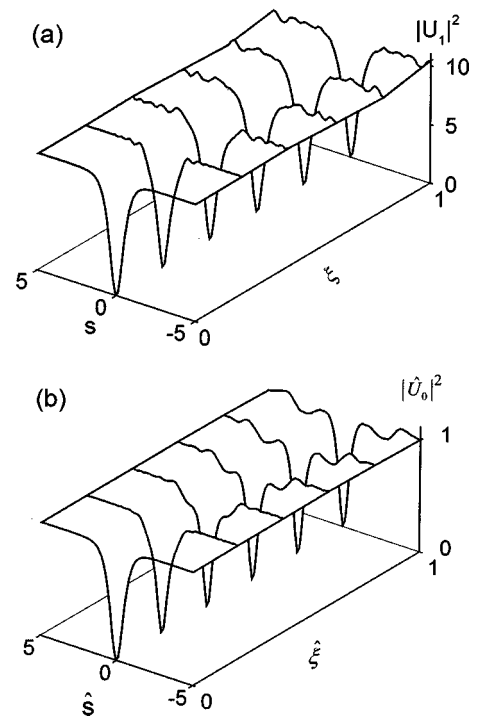


FIG. 7. Dynamical evolutions of the two dark solitary states U_1 and \hat{U}_0 in a biased series SBN crystal circuit. (a) U_1 in the crystal P and (b) \hat{U}_0 in the crystal \hat{P} .

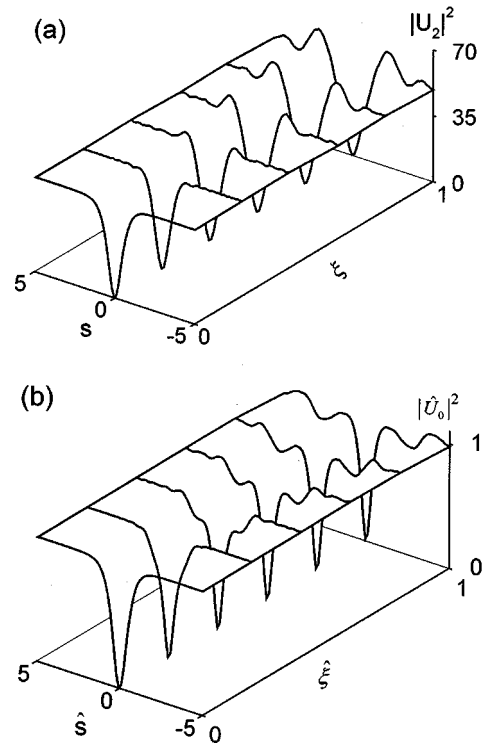


FIG. 8. Dynamical evolutions of the two dark solitary states U_2 and \hat{U}_0 in a biased series SBN crystal circuit. (a) U_2 in the crystal P and (b) \hat{U}_0 in the crystal \hat{P} .

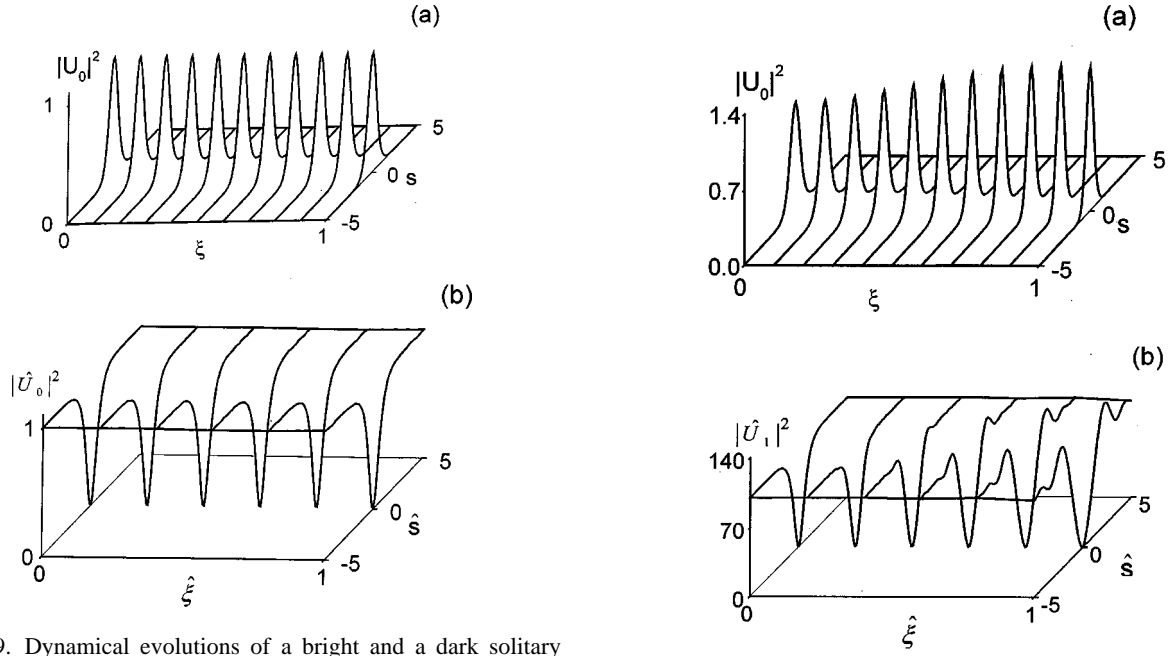


FIG. 9. Dynamical evolutions of a bright and a dark solitary states U_0 and \hat{U}_0 in a biased series SBN crystal circuit. (a) Bright soliton U_0 in the crystal P and (b) Dark soliton \hat{U}_0 in the crystal \hat{P} .

crystal P increases more, such as $U_2 = \sqrt{50}y_0(s)$, not only does U_2 tend to be unstable in the crystal P , but also \hat{U}_0 tends to be unstable in the crystal \hat{P} as shown in Fig. 8. These results are obtained by numerically solving Eq. (26) with $\beta = -0.335$ and $\rho = 50$ as well as Eq. (27) with $\hat{\beta} = -8.54$ and $\hat{\rho} = 1$, respectively.

If we change the incident beam of the crystal \hat{P} and keep the incident beam of the crystal P unchanged, such as, always taking U_0 as the incident beam for the crystal P but taking $\hat{U}_1 = \sqrt{10}\hat{y}_0(\hat{s})$ or $\hat{U}_2 = \sqrt{50}\hat{y}_0(\hat{s})$ as the incident beam for the crystal \hat{P} , some similar results can be obtained. The above results mean that, for a dark-dark separate screening soliton pair, a dark soliton can affect the evolution and stability of the other dark soliton by light-induced current. For a given biased series PR crystal circuit, whether an optical beam can evolve into a stable dark soliton in a crystal depends not only on the parameters of that optical beam, but also on the parameters of the other optical beam in the other crystal.

B. Bright-dark screening soliton pairs

Let us consider that a bright and a dark solitary beams evolve in a biased series SBN crystal circuit as shown in Fig. 1(b) with $E_A = 10^4$ V/m and $\hat{E}_A = -10^4$ V/m. The circuit has the same parameters as above. First, we consider the evolutions of two previously found solitary states as the incident beams with the input intensities $I_0 = I_d$ and $\hat{I}_\infty = \hat{I}_d$, respectively. If the crystal P supports the bright soliton, we have $I_\infty = 0$. The field profiles of the two solitary states, denoted here also by $y_0(s)$ and $\hat{y}_0(\hat{s})$, can be determined by solving Eq. (37) with $\beta = 5.92$ and $r = 1$ as well as Eq. (38) with $\hat{\beta} = -2.96$ and $\hat{\rho} = 1$, respectively. Therefore, we get a bright

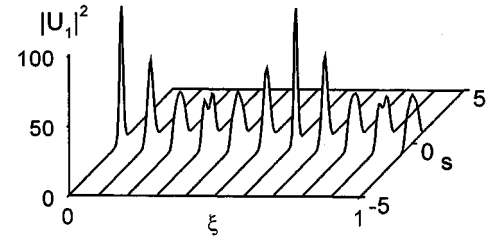


FIG. 10. Dynamical evolutions of three optical beams U_0 , U_1 , and \hat{U}_1 in a biased series PR crystal circuit. (a) Bright solitary state U_0 in the crystal P , (b) dark solitary state \hat{U}_1 in the crystal \hat{P} , and (c) bright solitary state U_1 in the crystal P .

and a dark solitary states $U_0 = \sqrt{1}y_0(s)$ and $\hat{U}_0 = \sqrt{1}\hat{y}_0(\hat{s})$, respectively. Taking the two solitary states as the input beams, their evolutions in the circuit are investigated by numerically solving Eq. (26) with $\beta = 5.92$ and $\rho = 0$ as well as Eq. (27) with $\hat{\beta} = -2.96$ and $\hat{\rho} = 1$. As expected, our results confirm that the two solitary states remain invariant with propagation distance as shown in Fig. 9.

We then consider the stabilities and the coupling effects between two solitary beams in the circuit. To do so, we follow the evolution of an optical beam in the crystal \hat{P} with an incident beam \hat{U}_1 whose field profile is still $\hat{y}_0(\hat{s})$, but its maximum amplitude is $\sqrt{100}$, i.e., $\hat{U}_1 = \sqrt{100}\hat{y}_0(\hat{s})$ and, simultaneously, we observe the evolution of $U_0 = \sqrt{1}y_0(s)$ in the crystal P . Obviously, \hat{U}_1 is not a solitary state supported by the crystal \hat{P} , whereas U_0 is still a solitary state supported by the crystal P . The evolutions of U_0 and \hat{U}_1 are investigated by numerically solving Eq. (26) with $\beta = 8.79$ and $\rho = 0$ as well as Eq. (27) with $\hat{\beta} = -0.087$ and $\hat{\rho} = 100$, respectively, as shown in Fig. 10. As we can see, not only does \hat{U}_1

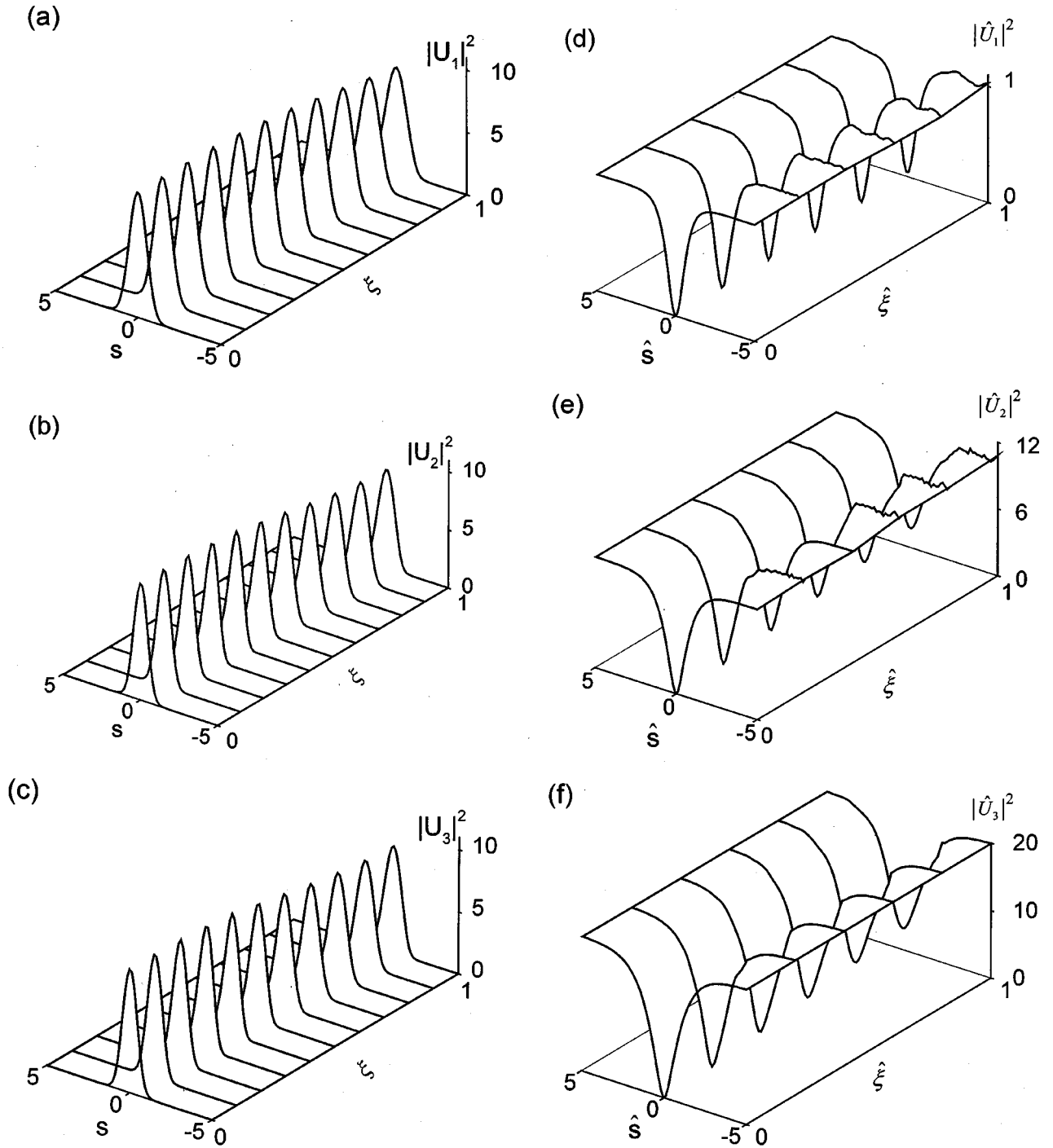


FIG. 11. The self-deflection of three bright-dark soliton pairs in a biased series SBN crystal circuit. (a)–(c) Bright solitons U_1 , U_2 , and U_3 in the crystal P . (d)–(f) Dark solitons \hat{U}_1 , \hat{U}_2 , and \hat{U}_3 in the crystal \hat{P} .

tend to be unstable in the crystal \hat{P} , but also U_0 cannot remain invariant with propagation distance and tries to evolve into a different solitary wave in the crystal P . If we change the incident beam of the crystal P and keep the incident beam of the crystal \hat{P} unchanged, such as, taking \hat{U}_0 as the incident beam for the crystal \hat{P} and taking $U_1 = \sqrt{100}y_0(s)$ as the incident beam for the crystal P , the evolutions of U_1 and \hat{U}_0 are obtained by solving Eq. (26) with

$\beta=5.92$ and $\rho=0$ as well as Eq. (27) with $\hat{\beta}=-2.96$ and $\rho=1$. The results are shown in Fig. 10(c) for U_1 and Fig. 9(b) for \hat{U}_0 . As we can see, though U_1 tends to be unstable in the crystal P , the evolution of \hat{U}_0 remains unchanged. The above results mean that for a bright-dark separate screening soliton pair, the dark soliton can affect the evolution and the stability of the bright soliton by the light-induced current, whereas the bright soliton cannot affect the dark soliton.

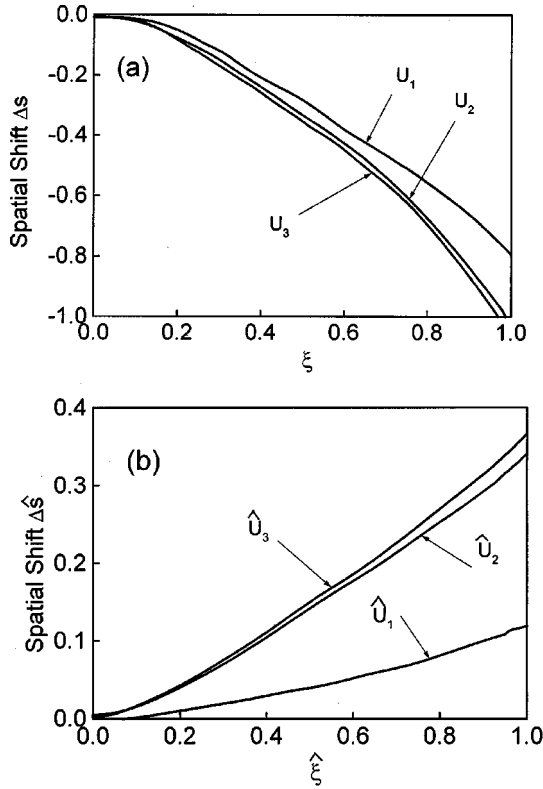


FIG. 12. The evolution of the spatial shift concerning with the results in Fig. 11. (a) The three bright solitons in the crystal P . (b) The three dark solitons in the crystal \hat{P} .

C. Bright-bright soliton pairs

As described above, for a bright-dark separate screening soliton pair, when the spatial extent of the optical wave is much less than the width of the crystal, the bright soliton cannot affect the dark soliton by the light-induced current. For a bright-bright screening soliton pair, this character holds valid if the condition is still satisfied, as a result, a bright soliton cannot affect the evolution and stability of the other bright soliton by the light-induced current. In other words, changing the input intensity of a bright soliton cannot affect the evolution and stability of the other bright soliton. However, for a bright-bright soliton pair, the dark irradiances will play a key role in the coupling effects between the two bright solitons. To be limited by the space, the coupling effects resulting from the dark irradiances will be discussed elsewhere.

V. SELF-DEFLECTION OF SEPARATE SCREENING SOLITON PAIRS AND COUPLING EFFECTS

It is an interesting topic whether the self-deflection of a soliton can be affected by the other soliton in a separate screening soliton pair. Obviously, this phenomenon maybe occurs in dark-dark or bright-dark soliton pairs. Here we take our attention on the effect of the dark soliton on the self-deflection of the bright soliton in a bright-dark screening soliton pair. To do so, we take the configuration shown in Fig. 1(b) with $E_A = 10^4$ V/m and $\hat{E}_A = -10^4$ V/m to support

the bright-dark screening soliton pair. Two SBN crystals are taken as the crystals P and \hat{P} , respectively, with the same parameters as above. Therefore, the diffusion coefficient can be calculated as follows: $\gamma = \hat{\gamma} = 0.56$.

Three bright-dark soliton pairs $U_j = \sqrt{r}y_j(s)$ and $\hat{U}_j = \sqrt{\rho}\hat{y}_j(\hat{s})$, $j=1,2,3$, are taken to be the input beams with the parameters $r=10$, $I_\infty=0$, (1) $\hat{I}_\infty=\hat{I}_d$; (2) $\hat{I}_\infty=10\hat{I}_d$, and (3) $\hat{I}_\infty=20\hat{I}_d$. From Eqs. (20) and (21) as well as $\beta = g\sigma E_A$ and $\hat{\beta} = \hat{g}\hat{\sigma}\hat{E}_A$, we have (1) $g=\frac{2}{3}$, $\hat{g}=\frac{1}{3}$, $\beta=5.92$, and $\hat{\beta}=-2.95$; (2) $g=\frac{11}{12}$, $\hat{g}=\frac{1}{12}$, $\beta=8.14$, and $\hat{\beta}=-0.74$; (3) $g=\frac{21}{22}$, $\hat{g}=\frac{1}{22}$, $\beta=8.44$, and $\hat{\beta}=-0.044$. The field profiles $y_j(s)$ and $\hat{y}_j(\hat{s})$ can be determined from Eqs. (37) and (38) with these parameters. The evolutions of the three bright-dark soliton pairs in the biased series SBN crystal circuit, including the process of self-deflection, can be investigated by numerically solving Eq. (26) with $\gamma=0.56$, $\rho=0$ and (1) $\beta=5.92$, (2) $\beta=8.14$, and (3) $\beta=8.44$ as well as Eq. (27) with $\hat{\gamma}=0.56$ and (1) $\hat{\rho}=1$, $\hat{\beta}=-2.95$, (2) $\hat{\rho}=10$, $\hat{\beta}=-0.74$, and (3) $\hat{\rho}=20$, $\hat{\beta}=-0.044$. The envelope evolutions of the three soliton pairs are shown in Fig. 11 and the associated spatial shift evolutions of the three soliton pairs are shown in Fig. 12. As we can see that the three dark solitons have three different bending angles, which is reasonable because the solitary beam with different input intensity has different bending angle [18–21]. However, the three bright solitons have three different bending angles although they have the same input intensity. In fact, to increase the input intensity of the dark soliton results in enhancing the value of β , and then increasing the bending angle of the bright soliton because the angle varies directly with β [18–21].

We also investigate the self-deflection of a dark-dark soliton pair. Our results show that a dark soliton can affect the self-deflection of the other dark soliton by the light-induced current. In fact, in the biased series SBN crystal circuit, the coupling electronically between the two crystals results in the bias voltage of each crystal changes with the input intensity of the dark soliton. Therefore, when the input intensity of a dark soliton changes, not only will the self-deflection of the dark soliton change, but the self-deflection of the other dark or bright soliton will also change.

VI. CONCLUSIONS

In this paper we investigate the problem of two one-dimensional optical beams propagating in the two PR crystals connected electronically by electrode leads in a chain with a bias source. The main results of this paper are, first, the detailed derivation of a system of two coupled equations that completely describes nonlinear propagation of two optical beams in a biased series PR crystal circuit and, second, the numerical analyses and detailed discussion of the interaction between the two solitons in a separate screening soliton pair, which result from the light-induced current, and the effects of the interaction on the spatial profiles, dynamical evolutions, stabilities, and self-deflection of the two solitons.

Because of both bright and dark screening solitons are

possible in a biased series PR crystal circuit, there are three types of separate screening soliton pair: dark-dark, bright-dark, and bright-bright. Unlike a screening soliton in a single biased PR crystal, in which the character of the soliton is determined only by the parameters of the single crystal, for a separate screening soliton pair in a biased series PR crystal circuit, the spatial profile, dynamical evolution, stability, self-deflection, etc., of any soliton in the soliton pair are determined by the parameters of the two crystals. The two solitons in a soliton pair can interact each other and the interaction can affect the spatial profiles, dynamical evolutions, stabilities, and self-deflection of the two solitons. The coupling effects can result from both the light-induced and dark currents

For a separate screening soliton pair form in a biased series PR crystal circuit, because the two PR crystals are connected electronically, changing the input intensity of a crystal, not only will the characters the soliton formed in that crystal change, but also the characters of the other soliton formed in the other crystal will change. However, only the dark soliton can affect the other soliton. The asymmetry comes from our results determined under the limit of the spatial extent of the optical wave being much less than the width of the crystal. In this limit, the light-induced current from a bright soliton is too weak to affect the other soliton, whereas one from a dark soliton is strong enough to affect the other soliton. As a result, for a bright-dark soliton pair, the dark soliton can affect the bright one by the light-induced current, but the bright soliton cannot affect the dark one. This unilateral effect may be useful in some applications, such as

a unidirectional optical coupler. Furthermore, we can think of a biased series PR crystal circuit as a system with two optical input signals and two optical output signals. If the circuit supports a bright-dark screening soliton pair, when the input signal of the dark soliton changes, the two output signals will change simultaneously, whereas when the input signal of the bright soliton changes, only the output signal of the bright soliton will change. This property may be used in optical switching technology. Another interesting phenomenon can also occur for a bright-dark soliton pair, i.e., the self-bending angle of the bright soliton can be controlled by the input intensity of the dark soliton. Perhaps a novel optical deflector could be made based on this principle.

Although the voltage measured between the two electrodes of the two crystals will decrease or increase if a resistor or a second voltage source is placed between the two crystals, the conclusions obtained in this paper are valid whether the resistor or the second voltage source is placed or not. The types of separate screening soliton pairs will increase when there are more than two crystals in the circuit. For example, there are four types of separate screening soliton pairs: bright-bright-bright, dark-dark-dark, bright-bright-dark, bright-dark-dark if three crystals are connected in the circuit.

ACKNOWLEDGMENT

The National Natural Science Foundation of China has supported this research under Grant No. 10174025.

-
- [1] Mordechai Segev, Bruno Crosignani, Amnon Yariv, and Baruch Fischer, *Phys. Rev. Lett.* **68**, 923 (1992).
 - [2] Galen C. Duree, Jr. *et al.*, *Phys. Rev. Lett.* **71**, 533 (1993).
 - [3] M. Segev, G. C. Valley, Bruno Crosignani, Paolo Diporto, and Amnon Yariv, *Phys. Rev. Lett.* **73**, 3211 (1994).
 - [4] D. N. Christodoulides and M. I. Carvalho, *J. Opt. Soc. Am. B* **12**, 1628 (1995).
 - [5] George C. Valley, M. Segev, Bruno Crosignani, Amnon Yariv, and M. C. Bashaw, *Phys. Rev. A* **50**, R4457 (1994).
 - [6] M. Segev, George C. Valley, M. C. Bashaw, M. Taya, and M. M. Fejer, *J. Opt. Soc. Am. B* **14**, 1772 (1997).
 - [7] Jinsong Liu and Keqing Lu, *J. Opt. Soc. Am. B* **16**, 550 (1999).
 - [8] Jinsong Liu, *Chin. Phys.* **10**, 1037 (2001).
 - [9] M.-F. Shih, M. Segev, G. C. Valley, G. Salamo, B. Crosignani, and P. Di Porto, *Electron. Lett.* **31**, 826 (1995).
 - [10] M. Taya, M. Bashaw, M. M. Fejer, M. Segev, and G. C. Valley, *Phys. Rev. A* **52**, 3095 (1995).
 - [11] D. N. Christodoulides, S. R. Singh, and M. I. Carvalho, *Appl. Phys. Lett.* **68**, 1763 (1996).
 - [12] M. Shih and M. Segev, *Opt. Lett.* **21**, 1538 (1996).
 - [13] Z. Chen, M. Segev, T. H. Coskun, D. N. Christodoulides, and Y. S. Kivshar, *J. Opt. Soc. Am. B* **21**, 3066 (1997).
 - [14] W. Krolikowski and S. A. Holmstrom, *Opt. Lett.* **22**, 369 (1997).
 - [15] A. V. Mamaev, M. Saffman, and A. A. Zozulya, *J. Opt. Soc. Am. B* **15**, 2097 (1998).
 - [16] Z. Chen, M. Acks, E. A. Ostrovskaya, and Y. S. Kivshar, *Opt. Lett.* **25**, 417 (2000).
 - [17] Chunfeng Hou, Zhongxiang Zhou, Xiudong Sun, and Baohong Yuan, *Optik (Stuttgart)* **112**, 17 (2001).
 - [18] Jinsong Liu and Zhonghua Hao, *J. Opt. Soc. Am. B* **19**, 513 (2002).
 - [19] Jinsong Liu and Zhonghua Hao, *J. Mod. Opt.* **48**, 1803 (2001).
 - [20] Jinsong Liu and Zhonghua Hao, *Phys. Lett. A* **285**, 377 (2001).
 - [21] M. I. Carvalho, S. R. Singh, and D. N. Christodoulides, *Opt. Commun.* **120**, 311 (1995).